I'MRT MATRIXX ARRAY CHARACTERIZATION AND SPATIAL MODIFICATION SIMULATIONS IN INTENSITY MODULATED RADIATION THERAPY (IMRT) AT 6 MV PHOTON BEAM IN NASOPHARYNX CANCER

by

SALEH ABDULLAH ALASHRAH

Thesis submitted in fulfillment of the requirements for degree of Doctor of Philosophy

December 2011

Acknowledgements

First of all, I would like to express my acknowledgement to my supervisor, Prof. Madya Dr. Sivamany Kandaiya, for her countless effort in guiding me throughout this research. I also thank her for taking a lot of effort to go through my research and providing me with a lot of information and suggestion. Without her, the study will never go this far.

Thanks to the physicist team as well as to the whole staff in the Radiology and Oncology Department of the Mt Miriam Hospital in Penang. Special thanks I intend to Dr. Soon Keong Cheng, Mr. Liang Soo Lum, Miss Joon Ching Tan, Mr. Tan Zi Xiang, Miss Wei Lyn Keh and Mr.Yong. Many thanks for the provision of the facilities used throughout the progress of this thesis.

Thanks to the physicist team in Department of Biomedical Physics in King Faisal special Hospital and Research Center (KFSH&RC) in Riyadh. Special thanks to Dr. Belal A. Mofta, Mr. Mammon Shehadeh and Mr. Abdullah Al Kafi. The use of the LINAC and the 2D array in this thesis is gratefully acknowledged. I want to thank Alqassim University for the financial support for my Ph.D programme.

I would like to express my gratitude to all those who gave me the possibility to complete this thesis. Many thanks for Dr. Yoon Tiem Leong and Dr. Eid Abdel_Munem throughout the progress of this thesis. I want to thank the biophysics and medical physics laboratory assistants: En. Azmi and En. Yahya for their technical support and help. I would like to thank my colleagues, Ying Chee Keat,

Yahye Abbas Amin, Khalid Saleh Ali Aldroobi and Dr. Ahmed Al Halmi for their support and help.

I would also like to express my acknowledgement to my family, especially my mother and father, who give me countless support and encouragement for this thesis. I would like to give my special thanks to my wife Hissah whose patient love enabled me to complete this work. I also thank my wonderful children: Abdullah, Hanin, Omar, and our new addition Mohammad, for always making me smile and for understanding on those weekend mornings when I was working this thesis instead of playing.

Table of Contents

LIST OF APPLICATION AND SEMINARS

List of tables

List of Figures

List of Abbreviations

1D, 2D ,3D	One, two and three dimensional axis respectively
3DCRT	three dimensional conformal radiation therapy
ACR	American College of Radiology
CM	Component modules
CT	Computed Tomography
DAO	Direct aperture optimization
DAVID	Device for the advanced verification of IMRT deliveries
DBS	Directional bremsstrahlung splitting
DICOM	Digital Imaging and Communications in Medicine
DMLC	sliding window IMRT technique
DTA	Distance to agreement
DVHs	dose volume histograms
EGS	Electron Gamma Shower
EPIDs	Electron portal imaging devices
EPOM	Effective point of measurement
FWHM	Full width at half maximum
IAEA	International Atomic Energy Agency
ICRU	International Commission on Radiation Units and Measurement
IMAT	Intensity modulated arc therapy
IMRT	Intensity modulated radiation therapy
ISP	International Specialty Products
linac	linear accelerator
MLCs	multileaf collimator
MOSFETs	Metal oxide semiconductor field-effect transistors

MUs	Monitor units
NEMA	National Electrical Manufacturers Association
NPC	Nasopharyngeal carcinoma
OAR	Organs at risk
OD	Optical Density
PDD	Percentage depth dose
PTV	Planning target volume
QA	Quality assurance
RGB	Red, green, blue
RT	Radiation therapy
SAD	Source axis distance
SCASPH	Scatter sphere
SCC	a squamous cell carcinoma
SMLC	step and shoot IMRT technique
SSD	Source surface distance
TIFF	Tagged image file format
TLD	Themoluminescent dosimeters
TPS	Treatment planning system
TSET	Total skin electron treatment
WHO	World Health Organization
$\gamma(r_r)$	Gamma index

PENCIRIAN DAN SIMULASI PENGUBAHSUAIAN RUANG I'MRT MATRIXX ARRAY UNTUK SINARAN INTENSITI TERMODULAT TERAPI (IMRT) PADA 6 MV FOTON DALAM KARSINOMA NASOFARYNX

Abstrak

Dua jenis kebuk pengionan pixel 2D: I'mRT MatriXX dari Scanditronix-Wellhöfer dan Seven29^{TM} dari PTW-Freiburg dikaji dengan objektif untuk melaksanakan jaminan kualiti dengan pengesahan perancangan rawatan IMRT. Ukuran lokasi berkesan I'mRT MatriXX dan Seven29TM telah disahkan dan didapati bersetuju dengan spesifikasi pengguna. Kebolehulangan pengesan I'mRT MatriXX telah diuji untuk jangka masa pendek, sederhana dan panjang. Kelinearan dos dan pergantungan pada tenaga juga dianalisis. Hasil kajian menunjukkan bahawa dos adalah linear dan tindak balas array 2D tidak bergantung kepada tenaga. Kajian terhadap kesan saiz medan yang berbeza pada tindak balas bagi array 2D telah dilaksanakan dan dibandingkan dengan kebuk pengionan. Kadar dos adalah juga linear dengan indak balas array 2D.

Pengukuran profil untuk saiz medan 2, 5, 8 dan 10 cm^2 telah dilaksanakan dan banding dengan kebuk pengionan. Hasil kajian menunjukkan bahawa tindak balas bagi MatriXX I'mRT perlu diperbetulkan di bahagian penumbra. Walau bagaimanapun, profil sinaran yang diukur oleh Seven29^{TM} lebih bersetuju dengan profil yang diperolehi dari PTW 30006 berbanding dengan pengukuran menggunakan I'mRT MatriXX. Satu sebab utama adalah jarak diantara dua kebuk pengionan Seven29^{TM} adalah sama dengan lebar MLC di isotengah. Pelebaran sinaran dibahagian penumbra menggunakan I'mRT MatriXX bergantung kepada saiz

pengesan dan jarak pusat-ke-pusat antara pengesan. Untuk menyelesaikan masalah ini, kernel kesusutan dengan fungsi Lorentz telah dipilih untuk menyelesaikan profil dos yang sebenar dari kebuk pengionan (IC03) dengan menggunakan R2009a MATLAB untuk merapatkan profil dos dari array 2D I'mRT MatriXX dengan saiz medan dari 2 × 2 ke 20 × 20 cm^2. Filem Gafchromic (EBT2) dan simulasi Monte Carlo (EGSnrc (BEAMnrc / DOSXYZnrc) code) juga digunakan untuk mengesahkan profil dos yang sebenar. Persetujuan profil dos yang baik didapati antara I'mRT MatriXX, IC03, EBT2 filem dan simulasi Monte Carlo yang memerhati di kawasan kecerunan yang rendah. Kecerunan dos yang lebih curam didapati mempunyai persetujuan yang lebih baik diantara I'mRT MatriXX dan IC03 selepas penggunaan kaedah Lorentz kekusutan kepada IC03 data. Perbezaan peratus maksimum tempatan antara MatriXX I'mRT dan IC03 adalah kira-kira 50% sebelum pembetulan dan dikurangkan kepada 10% selepas pembaikan untuk 2 × 2 cm^2. Lima perancangan IMRT nasofarinks juga dikaji. Nilai-nilai pengukuran array 2D dibandingkan dengan nilai-nilai (convoved) dari taburan dos didalam sistem perancangan rawatan. Kadar lulus yang baik telah diperolehi dengan penggunaan dos profil silang perancangan rawatan 3% / 3 mm kriteria indeks gamma dari array I'mRT MatriXX apabila dibanding dengan selepas pembetulan kekusutan. Kekusutan boleh meminimumkan perbezaan profil sinaran yang disebabkan oleh kesan purata isipadu pengesan ImRT MatriXX.

Untuk mengkaji kesan kepada kepada dan leher di permukaan melengkung fantom semi silinder pun dibuat. Taburan dos dengan medan saiz yang berbeza dan tiga rancangan karsinoma nasofarinks (NPC) IMRT diukur dengan model fantom semi silnder dan model fantom air dengan menggunakan array 2D pixel kamar pengionan I'mRT MatriXX. Persetujuan yang baik diantara I'mRT MatriXX ukuran

dan hipotesis TPS dengan kesauran pelan yang diperiksa (γ-indeks <1 93% piksel) dan perbezaan maksimum antara kedua-dua model fantom berada dalam lingkungan 3%.

I'MRT MATRIXX ARRAY CHARACTERIZATION AND SPATIAL MODIFICATION SIMULATIONS IN INTENSITY MODULATED RADIATION THERAPY (IMRT) AT 6 MV PHOTON BEAM IN NASOPHARYNX CANCER

Abstract

Two types of 2D pixel ionization chambers: I'mRT MatriXX from Scanditronix- Wellhöfer in Mount Mariam Hospital and Seven29^{TM} from PTW-Freiburg in King Faisal special Hospital and Research Center (KFSH&RC) in Riyadh were studied with the objective to implement for quality assurance in IMRT treatment plan verification. The effective point measurement of the I'mRT MatriXX and Seven29^{TM} were verified and it agreed with the manual specifications. The reproducibility of the I'mRT MatriXX detector was tested for the short-, medium- and long-term. The reproducibility was within 1.9%. Dose linearity and energy independence were also analyzed. The results showed that the dose was linear and the response of the 2D arrays was independent of energy. The effect of different field sizes on the response of the 2D arrays was performed and compared with the ionization chambers. The dose rate was also linear with the response of the 2D arrays. The profile measurements for field sizes 2×2, 5×5, 8×8 and 10×10 cm^2 were performed and compared with those obtained using the ionization chamber. The results showed that the response of the I'mRT MatriXX should be corrected in the penumbra region especially for small field sizes such as 2×2 and 3×3 cm^2. However, the beam profiles measured by Seven29^{TM} better matched profiles obtained from PTW 30006 compared to those measured using I'mRT MatriXX. One main reason is that the distance between two ionization chambers of Seven29^{TM} matches the width of MLCs at the isocenter.

Beam broadening in the penumbra region using I'mRT MatriXX depends on the detector size and the center-to-center distance between detectors. To solve this problem, a convolution kernel which is a Lorentz function was chosen to convolve the true dose profile from an ionization chamber (IC03) using the MATLAB R2009a to closely fit the dose profile from the 2D array I'mRT MatriXX for field sizes from 2×2 to 20×20 cm^2. Gafchromic film (EBT2) and Monte Carlo simulation (EGSnrc (BEAMnrc/DOSXYZnrc) code) were also used to verify the true dose profile. Good agreement in the dose profiles between I'mRT MatriXX, IC03, EBT2 film and the Monte Carlo simulation were observed in the low gradient region. In the steeper dose gradients better agreement between I'mRT MatriXX and IC03 was obtained after the Lorentz convolution method was applied to the IC03 data. The maximum local percentage difference between the I'mRT MatriXX and IC03 was about 50% before correction and reduced to 10% after convolution for 2×2 cm^2. Five nasopharynx IMRT plans were also studied. The measured values of the 2D array were compared with the convolved values of dose distribution from treatment planning system. Using the 3%/3 mm gamma index criteria good passing rates were obtained from the I'mRT MatriXX array when compared to cross dose profile plans from the treatment planning system after convolution correction. Convolution can minimize the difference in the beam profiles which occur due to volume averaging effect of the I'mRT MatriXX detector.

To study the effect of the curved surface of the head and neck, a semi cylindrical phantom was designed. Dose distribution of difference field sizes and three nasopharyngeal carcinoma (NPC) IMRT plans were measured in a semi cylindrical phantom and a flat slab solid water phantom using the 2D array pixel ionization chambers I'mRT MatriXX. A good agreement was found between I'mRT

MatriXX measurements and TPS predictions for all the examined plans (γ-index <1 for 93% of pixels) with a maximum difference between both the phantoms being within 3%.

CHAPTER 1

INTRODUCTION

1.1 Cancer

Cancer is a general word for diseases involving malignant tumors or growth caused when cells multiply without control. This destroys healthy tissues. It is the third most common cause of certified deaths in hospitals in Malaysia according to the Ministry of Health Malaysia (www.moh.gov.my). The World Health Organization statistics (WHO) shows that cancer accounted for 7.9 million deaths in 2007 (13% of all deaths worldwide) and predicted about 12 million in 2030. The most common cancers for men are lung, prostate, colon, head and neck, and bladder whereas for women are breast, uterus, colon, lung and ovary (Lemoigne and Caner, 2009).

1.2 Head and neck cancer

Head and neck cancer represents a difficult collection of tumors involving mucosal surfaces of the upper aero-digestive tract (Adelstein, 2005). Cell carcinoma of the head and neck affects more than 40,000 people each year in the U.S. This represents 4% to 5% of the total number of cancers diagnosed per annum and at least 13,000 people each year die of this disease (Brockstein and Masters, 2003). Carcinomas of the nasopharynx are more frequently diagnosed as head and neck malignancies in southeast Asia. Nasopharyngeal carcinoma (NPC) is a squamous cell carcinoma (SCC) that usually develops around the ostium of the Eustachian tube in the lateral wall of the nasopharynx (Sham et al., 1990). The first publication of 14 cases of NPC was in 1901 and characterized clinically in 1922 (Wei and Sham

2005). However, they represent a relatively rare disease in western countries (Lu et al., 2009). The Chinese had the highest incidence of NPC in Malaysia (Armstrong,1974).

According to WHO, NPC is classified into three types, WHO type 1 is keratinizing SCC, WHO type 2 is transitional cell and WHO type 3 is undifferentiated. WHO type 1 is similar in appearance to SCC in other sites throughout the upper aero-digestive tract. The other two types of NPC are nonkeratinizing and represent less differentiated forms of NPC. These undifferentiated forms, WHO types 2 and 3, are more common in the endemic region.

The incidence of NPC is lower than $1/10^5$ in most areas. High-incidence areas are centralized in the southern part of China (including Hong Kong) as shown in table 1.1. The highest incidence is found in Guangdong province, and the incidence in male can reach 20–50/100000 (Wei and Sham, 2005, Lu et al., 2009). Furthermore, the incidence of NPC is higher in male than in female and the ratio is 2-3: 1 (Parkin et al., 2002, Wei and Sham, 2005). Dietary as well as genetic factors play a role in the development of NPC (Bland et al., 2001). The incidence of NPC increases with age after 30 years and the peak is between 40 and 59 years in the high incident areas (Lu et al., 2009). Patients with WHO types 2 and 3 have a significantly higher 5- year survival rate (60% to 70 %) compared to patients with WHO type 1, keratinizing SCC (20% 5-year survival) (Wen-Zhan et al., 1989). The factor that has the most serious impact on survival is the presence and the characteristic of the lymph node. The head and neck region has a rich network of lymphatic vessels and SCC originated from the head and neck area including NPC

can metastasize to regional cervical neck lymph nodes even in its early stages. Therefore, understanding of the normal anatomy of the neck lymph nodes is crucial for the treatment of head and neck cancers. To ensure effective communication, a standard terminology is needed in the discussion of the complex lymph node regions. Various classifications have been developed for this purpose as shown in table 1.2 and figure 1.1 (Lu et al., 2009). The mere presence of regional lymph node involvement, especially nodal involvement that is large, is related to poor survival (Bland et al., 2001).

The age-standardized incidence (cancer) rate (ASR) is defined as the ratio of the number events (cancer) rate in a population being studied during a certain time period to the age distribution of an estimated standard population size through that time period (Parkin et al., 2002). Cancer rates change with sex, age, time and a number of other variables. The age-standardized incidence rate is expressed as the number of new cases per 100 000 person-years. The calculation can be expressed as follows (Parkin et al., 2002):

$$ASR = \sum_i \left(\frac{d_i\, w_i}{y_i}\right) \qquad (1.1)$$

Where i is number in each age group, d_i is the number of cases in the i^{th} age group, y_i the population size in the i^{th} age group and w_i the weight applied for the i^{th} age group. The age-standardized incidence rate in table 1.1 was between 20 to 60 years for male and female.

Table 1.1: Incidence of nasopharyngeal carcinoma (NPC) in some cancer registries in the world in 1998-2002 (Lu et al., 2009)

Region and population	Age –standard incident rate (N,1/10^5)	
	Male	Female
China		
China Zhongashan	26.9	10.1
China Gaungzhou	22.2	9.8
China Hong Kong	17.8	6.7
China Shanghai	4.1	1.5
China Nangang District Harlin city	1.1	0.5
Southeast Asia		
Malaysia, Sarawak	15.0	6.5
Malaysia, Penang	9.3	3.3
Singapore	11.0	3.6
Singapore: Chinese	12.8	4.1
Singapore: Indian	1.8	0.1
Singapore: Malay	5.5	2.0
Philippines, Manila	5.8	2.4
Thailand, Chiang Mai	3.9	1.5
Thailand, Songkhla	2.7	0.9
Thailand, Lampang	2.5	1.5
USA		
USA, Hawaii: Chinese	9.9	1.1
USA, Hawaii: Filipino	3.3	1.3
USA, Hawaii: Hawaiian	2.0	0.2
USA, San Francisco: Chinese	8.1	4.0
USA, San Francisco: Filipino	3.1	1.0
USA, Los Angeles: Chinese	6.0	1.9
USA, Los Angeles: Filipino	3.8	0.8
Middle East/North Africa		
Algeria, Setif	5.4	1.7
Tunisia, Sousse	4.6	1.9
Uganda, Kyadondo	2.3	1.3
Kuwait: Kuwaitis	1.7	0.8
Europe		
Austria	0.4	0.2
Finland	0.3	0.1
Canada, Northwest Territories	4.3	1.3
USA, Alaska	1.5	0.9

Table 1.2: Staging of nasopharyngeal carcinoma. T describes the size of the tumor and whether it has invaded nearby tissue, N describes regional lymph nodes that are involved, M describes distant metastasis (spread of cancer from one part to another) (Lu et al.,2009, http://en.wikipedia.org).

T	M	N
Tx: tumor cannot be evaluated	Mx: distant metastasis cannot be evaluated	Nx: lymph nodes cannot be evaluated
T1: the tumor confined to the nasopharyn	M0: no distant metastasis	N0: tumor cells absent from regional lymph nodes
T2: tumor extends to soft tissues	M1: metastasis to distant organs (beyond regional lymph nodes)	N1: unilateral lymph node metastasis (at some sites: tumor spread to closest or small number of regional lymph nodes)
T3:tumor invades to bony structures		N2: bilateral lymph node metastasis<6 cm
T4: intracranial extension and/or involvement of cranial nerves		N3: tumor spread to more distant or numerous regional lymph nodes (>6 cm)

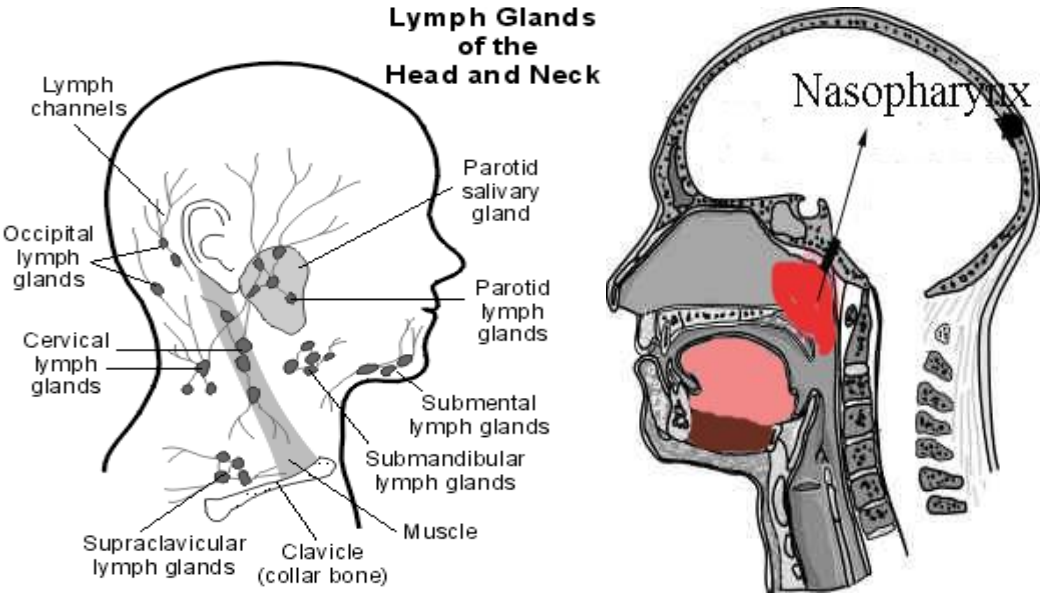

(a) (b)

Figure 1.1: (a) Lymph glands are joined together by a network of lymph channels. Lymph is a fluid that forms between the cells of the body (b) The lateral wall of nasopharynx (http://www.patient.co.uk/health/Lymph-Glands-Swollen.htm).

1.3 Role of radiation therapy in cancer treatment

Radiation therapy (RT) is the treatment of cancer patients with medium energy X-ray, high energy X-ray, gamma ray, proton, neutron or electron beams. Radiation may be delivered to tumor sites from an external source (i.e. teletherapy using linear accelerators) or at a short distance to the sites of tumor by using sealed radioactive sources called internal radiation therapy or brachytherapy (Khan, 2010). The biological effects of ionizing radiation originate primarily from the damage to the DNA of normal and tumor cells. Normal tissue cells suffer the same type of damage, but have better capacity of repair and control mechanisms. Any uncertainty on delivered dose may either result in an under dosage of the tumor or a complication for normal tissue. ICRU (the International Commission on Radiation Units and Measurements) No. 50 (ICRU, 1993) recommends a target dose uniformity within +7% and –5% of the dose delivered to a well-defined prescription point within the target. Patient setup, organ motion and deformation and machine uncertainty e.g. gantry angle and field sizes of the beam are the sources of the errors that degrade the exact dose delivery in PTV (planned target volume)(ICRU-83). With modern radiation therapy equipment and quality assurance program, the machine errors are small compared to patient setup deviations and organs motion. Therefore, treatment with external beam radiation therapy should be done carefully and precisely to achieve conformal dose distribution to the tumor site and sharp dose fall off to normal tissues.

Patients with malignant tumors can be treated with radiation therapy only or as a complement to other treatments such as surgery or chemotherapy as shown in Figure 1.2. Roughly one third of patients still fail locally after curative radiation

therapy (RT) but improvement in cancer cure has been observed in the last 2–3 decades. In order to improve local tumor control rates with RT the delivery of high doses to the tumor volume may be necessary (Lemoigne and Caner, 2009).

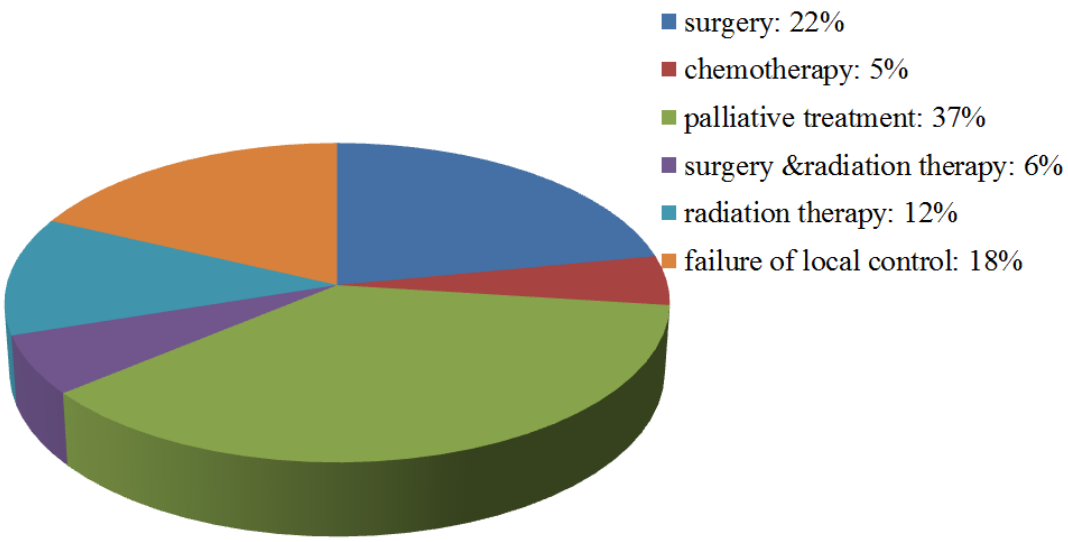

Figure 1.2: About half of all cancer patients receive radiation therapy, either as part of their primary treatment or in connection with recurrences or palliation. For Europe it was found that radiation therapy (alone/in combination) is successful in 18%. The failure rate of local tumor control is 18% (Lemoigne and Caner, 2009).

1.3.1 Three-dimensional conformal radiation therapy (3DCRT) of nasopharyngeal carcinoma

In three dimensional conformal radiation therapy (3DCRT) computers and special imaging techniques such as CT, MRI or PET scans are used to show the size, shape and location of the tumor as well as the surrounding organs. Three-dimensional imaging is necessary to define the target (tumor) and to distinguish it from normal tissues. Therefore, this technique is able to maximize the target dose and to minimize the dose to neighboring organs at risk by multiple radiation beams and multileaf collimator (MLCs). Once a suitable dose distribution has been reached, various other parameters relevant to the treatment can be used, such as monitor units and patient setup parameters. Modern, high-precision radiation therapy (RT)

techniques are needed in order to implement the goal of optimal tumor destruction and to deliver the minimal dose to the surrounding tissues.

Nasopharyngeal carcinoma (NPC) is highly sensitive to ionizing radiation and radiation therapy is the support treatment modality for non-metastatic diseases (Kam et al., 2003). For decades, NPC radiation therapy uses conventional treatment utilizing two-dimensional and lately three-dimensional techniques. Both techniques mainly use opposed lateral fields with or without an anterior field focused on the primary tumor (figure 1.3) (En-Pee et al., 1989, Waldron et al., 2003). The ability for 3DCRT to alter isodose lines was limited to shaping of field boundaries with MLCs or blocks, the use of wedges or compensators for missing tissues, and central blocks for shielding critical structures. Disease control using conventional radiation therapy techniques has been acceptable; however, insufficient dose to parts of the targets and insufficient protection of critical structures such as optic chiasm, middle/inner ear, eyes, spinal cord, and/or brainstem may result in reduced disease control in advanced NPC. There are limitations using 3DCRT such as:

i. Need a large number of beams unless target shape is very simple.
ii. Optimal beam angles often non-axial and difficult or impossible to use.
iii. In the head and neck area, there are a large number of sensitive tissues. Therefore, require few beam directions.
iv. No acceptable plan for concave target.

So, head and neck cancers, especially NPC is ideally suited for treatment with IMRT to spare critical normal structures and to have better target coverage (Laskar et al., 2008).

1.3.2 Intensity modulated radiation therapy (IMRT)

Intensity modulated radiation therapy (IMRT) is capable of generating complex three-dimensional dose distributions to conform closely to the target volume, even in tumors with concave isodose shapes (30% of tumors) (Nutting et al., 2000). It represents one of the most significant technical advances in radiation therapy (Ezzell et al., 2003). In the IMRT, the intensity of the incident fluence radiation field varies and each field consists of several small intensity modulated beams (beamlets) to match the projection of the planning target volume (PTV) as shown in figure 1.3. Hence, the fluence from each beam creates an acceptable uniform dose within the PTV and a low dose to OARs. The subsequent dose distributions from IMRT are highly conformal and unique. It can produce a concave dose distribution and results in steep dose gradients between planning target volumes (PTV) and organs at risk (OAR) (Nutting et al., 2000). An acceptable treatment plan is one in which planning target dose uniformity is within +7% and –5% of the dose delivered to a well defined prescription point within the target, and the doses to OAR are low. Therefore, by using this technique, it is possible to distribute the dose homogeneity to fit tumors with complex shape (e.g. concave shape) while sparing critical normal tissues (Dogan et al., 2002, Kam et al., 2003). The dose-volume histogram of the target volume and dose to the sensitive normal tissue structures was used to compare for a number of NPC carcinoma cases between IMRT treatment plans and 3DCRT treatment plans by many authors (Xia et al., 2000, Cozzi et al., 2001, Hunt et al., 2001, Kam et al., 2003, Poon et al., 2007). Their results showed that IMRT demonstrated better target coverage and sparing to a number of organs at risk (OAR) including parotid glands, brainstem, eye, middle and inner ear and spinal cord than that of 3DCRT.

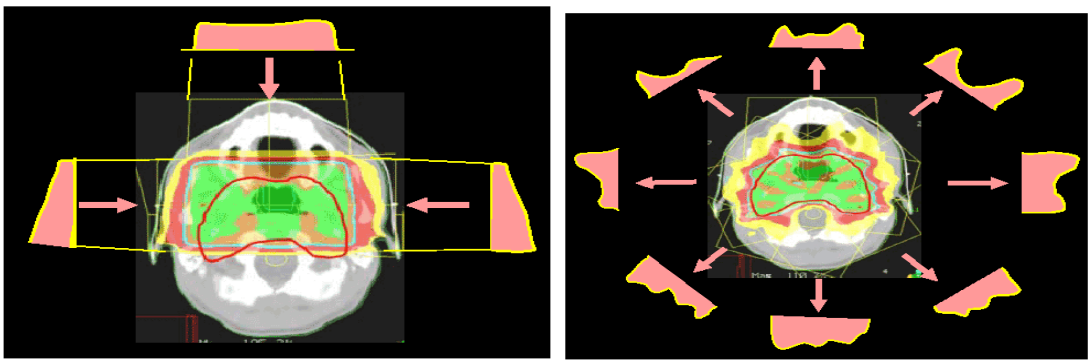

Figure 1.3: Comparison of 3DCRT (left) and IMRT (right). The IMRT beams can have highly non-uniform beam intensities (fluences) and are capable of producing a more concave-shaped absorbed-dose distribution (Butson et al., 2006b).

1.4 Treatment planning methods

The software code used to calculate dose distributions in a patient or a phantom is called the "treatment planning system" (TPS). There are two methods of TPSs. The first is named forward planning which is used in 3DCRT. In this method of treatment planning, the planner defines the beam parameters like beam directions, number of beams and size of the beam, collimator setting (position of MLCs), beam weight factors of each field, the use of wedges, compensators or blocks. Next, the dose is calculated using the treatment planning system. For the worse case, the planner shall modify some parameters of the beam manually till he gets a satisfactory plan (Eisbruch et al., 1998, Fogliata et al., 1999). The second method is named inverse planning which is used in IMRT. The inverse treatment planning is the method of planning where objectives such as target volumes and OARs are allowed for in automatic calculation of dose distribution according to a preselected algorithm. The algorithm is used to determine beam parameters like the number of beamlets, the positions of MLCs and the number of MUs in order to get a better dose distribution that corresponds as much as possible to the initially defined objectives.

In fact there is a large difference between the two treatment planning techniques: The forward planning is a manual iterative process by the planner till he obtains an acceptable result. In inverse treatment planning system, the planner instructs the PC what he would want to obtain a dose distribution for the target (tumor) and the OARs. The basic steps in IMRT treatment is shown in figure 1.4. The algorithm will carry out these objectives to obtain the desired dose distribution. The inverse treatment planning seems to be more efficient. However, one should be careful as it has many difficulties in comparison with forward planning. These difficulties include (Jiang et al., 2005):

i. Treatment time of a patient is more than 3DCRT.
ii. Increased quality assurance efforts.
iii. The leakage through tongue and groove could become significant in IMRT (Huq et al., 2002).
iv. Increased shielding requirements due to increased leakage radiation and neutron contamination.

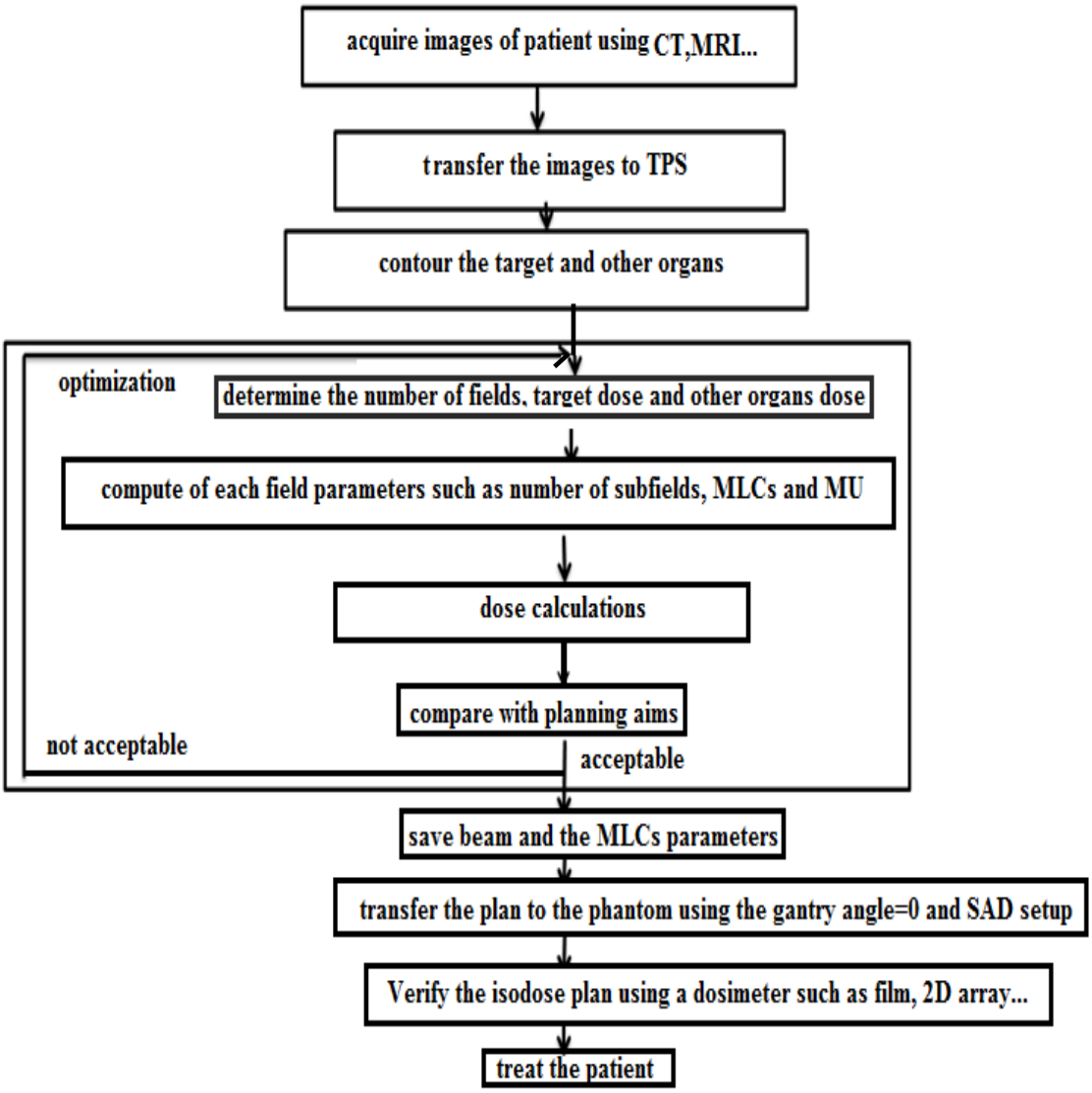

Figure 1.4: Flow chart of the steps in a IMRT treatment.

1.5 Different IMRT delivery techniques

All intensity modulated treatments are performed by changing the multileaf collimator MLC shape to irradiate different sections of the target volume. This is performed by changing the shape of sub-field and monitor units (dose) associated with each MLC segment. Different portions of the target are irradiated separately. The summation of these MLC patterns gives the total dose to the irradiated volume. This combination of beam angles, intensity of dose and MLC segments is designed to deliver highly conformal dose distributions (Wu et al., 2010). So, the multi-leaf

collimator (MLC) based IMRT techniques that are most currently used fall into three categories:

i. The segmented MLC (SMLC) mode, often referred to as the step and shoot mode.
ii. The dynamic MLC (DMLC) mode sometimes referred to as the sliding window mode.
iii. Intensity modulated arc therapy (IMAT)

In step and shoot technique, the beam is only turned on when the MLC leaves are stationary in each of the prescribed beamlet during delivery. The intensity modulated fields are delivered with a sequence of small segments or beamlets, each beamlet with a uniform intensity. To achieve maximum conform dose to the target volume 4 to 9 beam directions may be required depending on the complexity of the PTV (Jiang et al., 2005). Static IMRT technique is used in Mount Miriam Hospital in Penang Malaysia, for the treatment of different types of tumors especially NPC cases. The individual fields consist of 3 to 20 beamlets, which are delivered in succession. The number of beamlets result in an increase of treatment time for IMRT to about 2.5 times more than 3DCRT (Nutting et al., 2000). To reduce delivery times of inverse planning systems, direct aperture optimization (DAO) should be used. It is used to reduce the monitor units of the beamlet and/or reduce the number of beamlets (Ludlum and Xia, 2008, McGarry et al., 2011a, McGarry et al., 2011b).

In the dynamic MLC mode (dynamic IMRT) the delivery of the intensity modulated fields are carried out while the leaves of the MLC are moving during patient treatment in a dynamic way (figure 1.5). In this mode IMFs (intensity modulated fields) are created by means of moving corresponding leaves independently at different velocities as a function of time, while the beam is on. A

desirable dose can be obtained by changing the position and the speed of MLCs. The dynamic IMRT treatment time is much faster than static IMRT technique; typical delivery time for a five - field prostate treatment is 14 min (Nutting et al., 2000).

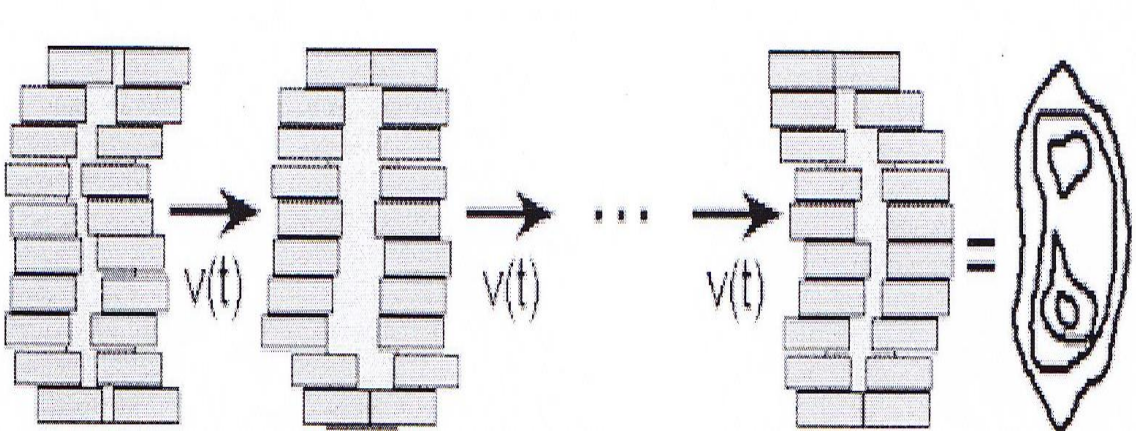

Figure 1.5**:** Dynamic IMRT technique.

The intensity modulated arc therapy (IMAT) delivery method uses the sliding window approach while the gantry rotates around the patient. The advantage of using IMAT technique includes faster delivery time than dynamic MLC (estimated at 5 – 10 min) and the use of fewer intensity levels than dynamic MLCs (Boyer and Yu, 1999). The sliding window IMRT and IMAT produce better target dose homogeneity compared to step and shoot IMRT (Wiezorek et al., 2011). The main difference between IMAT and IMRT is that IMRT consists of a few gantry angles with a number of beamlets for each beam direction while IMAT has a single MLC segment at each of the many beam directions. However, the segment shapes are restricted by the MLCs leaves and gantry rotation speeds. Figure 1.6 (a) and (b) show the distribution of beams and beamlets for the IMRT and the IMAT techniques, respectively (Wu et al., 2010). For IMRT, a few beams distributed around the patient, with number of beamlets associated with each beam (figure 1.6 (a)) while

figure 1.6 (b) shows many beams distributed around the patient with one MLC segment connected with one beam (IMAT).

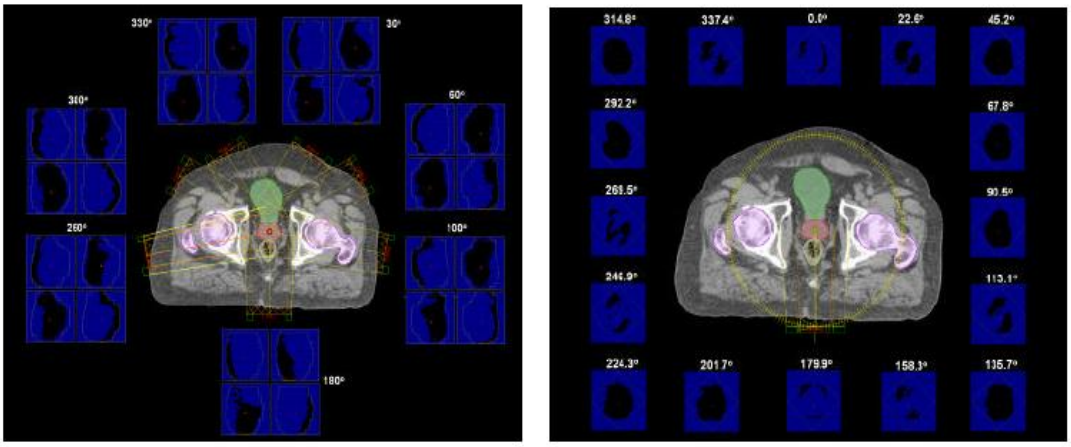

(a) (b)

Figure 1.6: Beams direction and beamlets for IMRT and IMAT distribute around a patient (Wu et al., 2010).

1.6 IMRT verification

A conformal treatment plan consists of two to four open fields, each with a homogeneous dose profile. These fields are applied from different directions. On the other hand, IMRT uses non-uniform radiation beam intensities which are determined using computer-based optimization techniques. The dose distribution on the target can be further shaped by modulating the intensity of each field used. Due to the complexity of the technique, verification of the dose delivery is important. In IMRT, it is necessary to verify the calculated dose distribution from TPS and the actual dose distribution in patient via phantom. There are several methods available for IMRT verification. The most widely used are films which have good spatial resolution but the films have to be calibrated against dose. Gafchromic films which were developed for industrial radiation monitoring have been refined for clinical radiation therapy dosimetry (Chu et al., 1990, Devic et al., 2004). These films are self-developing and require no physical/chemical processing. The optical density of the irradiated film is

measured using optical measuring systems such as densitometers and document scanners (Devic et al., 2005, Sankar et al., 2006). Electron portal imaging devices (EPIDs) do have good spatial resolution but require calibration and they age with radiation. EPIDs are available on treatment machines and are used for position verification of patients. EPID dosimetry using deconvolution methods are used to estimate dose in a patient (Wendling et al., 2006, Wendling et al., 2009). The 2-D detector array that can be placed on top of the treatment couch or attached to the accelerator head can improve verification time compared to film measurements. 2D array of pixel ionization chambers do have poorer resolution but provide direct measurement of dose without frequent calibration (Spezi et al., 2005, Herzen et al., 2007). The measurements are in real time.

1.7 Objectives of the study

1. To study the characteristics of a commercialized array of 2D pixel ionization chambers I'mRT MatriXX from Scanditronix Wellhöfer using Siemens Artist linac (6 and 10 MV) in Mount Mariam Hospital.
2. To implement I'mRT MatriXX for IMRT quality assurance in NPC IMRT treatment plan verification using Siemens Artist linac (6 MV).
3. To evaluate the capability of a commercialized array of 2D pixel ionization chambers Seven29^{TM} (PTW, Freiburg, Germany) in King Faisal Special Hospital with the objective to implement for IMRT quality assurance for NPC IMRT treatment plan verification on Varian linac 2300 EX (6 and 18 MV).
4. To correct the response of the I'mRT MatriXX in high gradient region using a convolution correction method.

5. To apply the convolution method to the true beam profile for different field sizes and IMRT plans measured using small ionization chamber (IC03) and gafchromic films (EBT2 films). The profiles were also calculated using Monte Carlo simulation EGSnrc (BEAMnrc/DOSXYZnrc).
6. To study the effect of irregular head and neck shape on a semi-cylindrical phantom designed for a number of NPC IMRT QA cases.

1.8 Contributions

From the characteristics of two types of 2D arrays (I'mRT MatriXX and Seven29^{TM}) the Seven29^{TM} was toward to be a better 2D array than MatriXX for IMRT QA. The distance between the centers of two adjacent chambers for seven29^{TM} is equal to the MLC width at the ioscenter plan whilst for I'mRT MatriXX, the distance is 0.762 cm.

A convolution kernel, a Lorentz function, was introduced to fit the response function of a finite size of a single detector in the I'mRT MatriXX. The convolution of the true dose profile with this function gave a better agreement with the MatriXX measured data. This function is simpler compared to a Gaussian function. Use of the convolution would better improve the TPS plans with MatriXX measured data. This would be necessary in NPC plans which have steep gradients.

However curved surfaces have little impact on TPS verification if the plans had been replanned on the phantom with curved contours.

1.9 Structure of the thesis

This thesis contains seven chapters having the common theme; evaluation of an array of 2D pixel ionization chambers (I'mRT MatriXX) for nasopharynx cases (NPC) in intensity modulated radiation therapy (IMRT) verification. Chapter 1 is the introduction on external NPC radiation therapy, spread of lymphatic routes of NPC anatomy, description of treatment types and the main objectives of this research.

Chapter 2 is a literature review on an array of 2D pixel ionization chambers for nasopharynx cases (NPC) in intensity modulated radiation therapy (IMRT) verification. It is divided into four categories: i) characteristics of 2D array detectors and film dosimeters and their implementation in IMRT QA, ii) detector size effects for small field sizes, iii) convolution correction method, iv) Monte Carlo Simulation EGSnrc (BEAMnrc/DOSXYZnrc). Chapter 3 describes the instrumentation utilized in this research. There are two main categories of instruments used, namely the detectors and their software with the ancillary equipment. The detectors employed include I'mRT MatriXX and Seven29^{TM}. The software of the I'mRT MatriXX is named OmniPro-I'mRT software and Seven29^{TM} has two softwares named MatrixScan software and VeriSoft software. Gafchromic films and two types of ionization chamber were also used. Two types of phantoms are described, namely the solid water phantom and the semi-cylindrical perspex phantom for NPC IMRT QA cases. The CT scan and linear accelerator (linac) are also described. Validation of the experimental work for dose calculations and measurements is provided in the following four chapters. Chapter 4 presents study of the characteristics of the 2D array (I'mRT MatriXX and Seven29^{TM}). Convolution method to correct detector response function for small fields in 2D array I'mRT MatriXX was applied in chapter 5. It includes measurements of beam profiles using gafchromic films and

Monte Carlo simulation. In chapter 6 a semi-cylindrical phantom was designed to study the effect of irregular head and neck shape for a number of NPC IMRT QA cases. Finally, chapter 7 the conclusion provides a summary of the major results and potential avenues for future work.

CHAPTER 2

LITERATURE REVIEW

2.1 Essentials of an ideal dosimeter

IMRT provides a significant improvement in the radiation dose distribution and is more advantageous for definitive therapy for non-metastatic NPC (Lu et al., 2009, Ezzell et al., 2003). However, IMRT produces complex treatment plans and delivery techniques. Hence, IMRT requires pre-treatment verification. Here the patient TPS plan is recalculated in a QA phantom and verified using a dosimeter. Different dosimeters such as ionization chamber dosimeters, thermoluminescent dosimeters (TLDs), metal oxide semiconductor field-effect transistors (MOSFETs), films (radiographic and gafchromic) , 2D array (pixel ionization chambers or diodes) and electronic portal imaging device (EPID) have been developed for the validation of IMRT treatment plans (Ezzell et al., 2003). An ideal dosimeter has some basic features that makes it suitable for comparison with TPS values (Butson et al., 2003, Wagter, 2004, Wilcox and Daskalov, 2007, Lemoigne and Caner, 2009). The basic features are as follows:

1. Reproducibility: In dosimetry, the uncertainty associated with the measurement is often expressed in terms of reproducibility and accuracy. Reproducibility is defined as the ability to get same results under similar conditions of measurement techniques. High reproducibility is associated with a small standard deviation in the distribution of the results in the measurements. Reproducibility includes systematic errors in a dosimetry device, electrometer leakage and repeated measurements.

2. Accuracy: The accuracy is the ability of the dosimeter to measure the delivered dose correctly and it matches the true value of the measured dose. The main disadvantage of this definition is that it requires the knowledge of the true value of dose. However, the true value is unknown exactly.
3. Absolute dose determination: An ideal dosimeter should measure the absolute dose (Gy) rather than relative dose (%). Normalization procedure can be used to convert relative dose to absolute dose (Wagter, 2004).
4. Dose distribution: The 3-dimensional (3D) measured dose distribution has to be "available" after IMRT treatment delivery to the dosimeter. Then dose volume histograms (DVHs) for planning can be compared to the DVHs of the measured dose distributions (Wagter, 2004).
5. Independent of beam direction: The ideal dosimeter response is independent of orientation of irradiation. This requirement is ideally met if the dosimeter is tissue equivalent and circular in shape (Wagter, 2004).
6. Dose and dose rate response: The response of an ideal dosimeter should be linear with either the dose or the dose rate. This is important when pulsed high-energy linear accelerators are used because pulses of high doses of radiation are delivered in short time periods.
7. Field size independence: An ideal dosimeter should be independent of the field size.
8. Energy independence: For an ideal detector, there should be no difference in the response of the dosimeter with varying energies of the incident beam. The smallest change in response of the dosimeter with radiation energy usually means that an effective atomic number of the dosimeter is close to the tissue.

9. Spatial resolution: Since the dose is a point quantity, the dosimeter should determine the dose from a very small volume (i.e. a point dosimeter should be used to have the value of the dose at a point). The position of the point where the dose is determined (i.e. its spatial location) should be well defined in a reference coordinate system. Practically, all dosimeters have a finite size and they can provide inaccurate readings of delivered dose in high-dose gradients such as the penumbral regions.
10. Detection time: The response of an ideal dosimeter should show the measured dose immediately after radiation.
11. Toxic hazards: An ideal dosimeter has low toxic hazards.
12. The cost: An ideal dosimeter should be reasonable in cost.
13. Ease of handling: An ideal detector would be simple to use and physically strong enough for clinical use on a routine basis without any physical limitations.

Obviously, not all dosimeters can satisfy all these characteristics. Therefore, the choice of a radiation dosimeter and its reader must be made sensibly, taking into account the requirements of the measurement conditions. Some physical characteristics of an ideal dosimeter listed above have been studied for dosimeters such as gafchromic films and 2D ionization chamber arrays used in IMRT pre-treatment verification.

2.2 Film dosimeters

2.2.1 Radiographic film

Film dosimetry is the traditional method of evaluating two dimensional (2D) dose distributions. In the past, a radiographic film is coated with silver halide, which

exhibits a strong photon energy dependence as it has a high atomic number (Z) due to silver halides (Cheung et al., 2006, Schneider et al., 2009). Hurter and Driffield investigated the response of the film to radiation in the 1890s, and the graph describing optical density (OD) versus the exposure or dose is called the H and D curve, in their honour. A more general term is named the characteristic curve (Bushberg, 2002). The characteristics of film response can be plotted in various ways. For example, dose vs. OD, log (dose) vs. OD, or log (dose) vs. log (OD) can be used. There are advantages to each of these plots. However, in radiation oncology the dose versus OD is most often used (Pai et al., 2007). The H and D curve typically has three sections: toe, gradient, and shoulder.

The response of the film is strongly dependent on the dose, dose rate and field sizes. Due to this dependence, no standard calibration curve (H and D) can be used to convert net optical density into dose for the same batch if the setup parameters are changed (e.g. field size, dose and energy of the beam) (Dogan et al., 2002, Fuss et al., 2007). It also means that the radiographic film is not an ideal dosimeter and is not used in situations where the dose distribution may vary sharply, e.g. penumbra regions and IMRT (Cheung et al., 2006). Most radiographic films have a relative short region of linear dose response in the calibration curve. For example, the saturation dose for XV2 Kodak film is about 100 cGy. The dose fraction of IMRT is usually from 1.8 to 2.2 Gy/fraction. Hence, IMRT dose distribution should be reduced by a factor 3-4 to be in the dose response region of XV2 films (Dogan et al., 2002). In a later EDR2 film the concentration of silver (cubic shape) is about 50% compared with that for X omat Kodak film. Therefore, the EDR2 film has a lower energy dependence compared with XV and X omat films. Its saturation dose is about 500 cGy to 600 cGy (Olch, 2002, San et al., 2005).

Therefore, EDR2 film has a lower sensitivity and it is possible to use it for IMRT verification. The reproducibility and accuracy of radiographic film was performed by several authors (Dogan et al., 2002, Childress et al., 2005, Suriyapee et al., 2008). They showed that EDR2, X omat and XV2 films were reproducible and accurate with a maximum difference of 1.5%. They used special developing processes otherwise higher inaccuracies can be expected (Suriyapee et al., 2008, Ferreira et al., 2009).

2.2.2 Gafchromic film

Presently, gafchromic film (Z_{effect}=6.0 to 6.98) has an important characteristic that is it is tissue equivalent. Its sensitive layer consists of an organic composition like carbon, hydrogen, oxygen, and nitrogen (Cheung et al., 2006, Butson et al., 2006b) and it is close to the effective atomic number of water (Z_{effect}=7.3) (Butson et al., 2006b). Like radiographic film, the gafchromic film can display dose distribution in two dimensions in radiation therapy verifications with high spatial resolution. There are several commercial gafchromic films used in radiation therapy such as HS, MD-55-2, MD-810, EBT and EBT2 film (figure 2.1). The gafchromic film has a high reproducibility (Thomas et al., 2003). The Gafchromic™ EBT was commercially released in 2004 and EBT stands for external beam therapy (Fiandra et al., 2006, Devic, 2010). Gafchromic film (EBT) is field size independent from 5×5 to 40×40 cm^2 and it can be used for measuring dose in small field sizes (0.5×0.5 cm^2) where ion chambers cannot work. For energy dependence, the variation in the range of photon energy from 50 kVp to 25 MV, EBT was <10% (Butson et al., 2006b, Fuss et al., 2007). Therefore, the gafchromic film (EBT) has weak energy dependence (Fiandra et al., 2006). Hence, a standard calibration curve of EBT film